

## EXPERIMENTAL VALIDATION WORK TO PROVE THE MASTER CURVE CONCEPT

**D. E. McCabe**

Metals and Ceramics Division, Oak Ridge National Laboratory  
Oak Ridge, TN 37831, USA

**M. A. Sokolov**

Metals and Ceramics Division, Oak Ridge National Laboratory  
Oak Ridge, TN 37831, USA

**Abstract.** *The introduction of elastic-plastic fracture mechanics and statistical methods into transition temperature characterization of ferritic steels has led to the Master Curve concept. Data scatter, specimen size effects, and a universal transition curve behavior have been identified and explained using a weakest-link statistical concept. This paper presents the experimental evidence to support these findings. However, the modeling that works successfully under most practical conditions does not apply under all scenarios. These limitations are currently being explored. The use of precracked Charpy specimens to produce viable fracture-mechanics data is one of the issues addressed.*

**Keywords:** *Master Curve, fracture mechanics, transition temperature*

### 1. INTRODUCTION

Fracture-mechanics analysis methods are currently being used to analyze nuclear reactor vessels under faulted conditions and for pressure/temperature combinations that are permitted during normal start-up and shutdown operations. Perhaps the most significant technical progress has been made during the past few years in improving knowledge of stress distributions during reactor upset transients, allowing more accurate stress-intensity-factor solutions for assumed crack sizes, shapes, and locations. However, the method used to establish fracture-mechanics-based fracture-toughness characterization of the materials being used has not kept pace with the analytical progress. Material fracture-toughness characterization has been handled by a semi-empirical scheme that was devised in the 1970–72 time-frame (EPRI, 1993). At that time there was very little experience to draw upon, and the fracture-toughness characterization scheme devised was approximate in nature; that is, the methodology could not be expected to be permanent. Some fracture-mechanics concepts developed for use on aerospace materials had been adopted from American Society for Testing and Materials (ASTM) standard method E 399 (ASTM 1982a), using  $K_{Ic}$  and adhering to its validity requirements. This approach required huge specimens of reactor pressure vessel (RPV) steels when testing was to be performed in the transition range. Also, data scatter among replicate tests could be substantial, and control of this scatter could not be achieved by constraint condition management of the type that had worked successfully on aerospace materials. The resolution for these difficulties was to develop two working postulates (WRC, 1972). One postulate was that a lower bound curve, drawn beneath a fairly substantial collection of valid  $K_{Ic}$  data, could be used as a universal curve. By implication,

this curve was expected to underlie the fracture-toughness data for all past and future production RPV steel plates and their weldments. It was also postulated that lower bound  $K_{Ic}$  estimates could be suitably indexed with respect to temperature by means of non-fracture-mechanics test methods (ASTM, 1982b; ASME, 1993). This approximate methodology has been in use with only minor modifications for almost 30 years.

New ideas began to emerge starting in about 1980, and there has been continuous progress made since, culminating recently in the Master Curve concept and ASTM standard method E 1921–97 (ASTM, 1998). Advanced statistical methods and improved understanding of elastic-plastic test methods have been coupled to define a transition curve that is derived using only fracture-mechanics-based test data. The uncertainties associated with the empirical postulates that had to be employed since the 1970s are eliminated. The reason for excessive data scatter even under controlled constraint conditions can now be explained. Specimen size effect on material fracture toughness is better understood. Consequently, the definition of a transition temperature for a given material can be stated in terms of the more accurate defining temperature,  $T_0$ . The key elements of the new technology are as follows.

1. Data scatter is recognized as resulting from randomly distributed cleavage crack-triggering sources contained within the typical microstructure of ferritic steel (Merkle et al., 1998). A three-parameter Weibull statistical model is used to suitably fit observed data scatter. Elastic-plastic fracture-toughness evaluation is expressed in units of a stress-intensity factor,  $K_{Jc}$ .
2. The J-integral at the point of onset of cleavage instability,  $J_c$ , is calculated first and converted into its stress-intensity factor equivalent as  $K_{Jc}$ . It has been proven that sufficient control of constraint can still be maintained with specimens that are one-fortieth the size required for validity by ASTM E 399.
3. The specimen size effect observed in transition-range testing is quite subtle, and the most accurate modeling of this effect uses a weakest-link assumption, derived from the item 1 observation (Landes and Shaffer, 1980). The recognition of this model enables conversion of  $K_{Jc}$  data obtained from specimens of one size to  $K_{Jc}$  data for specimens of another size.
4. Use of the above three items has made it possible to observe that most ferritic steels tend to conform to one universal transition curve shape. Hence the existence of a universal “Master Curve” could be demonstrated (Wallin, 1989). Although the Master Curve is based on one selected specimen size, the universality property seems to extend without modification to engineering applications.

The objective of this paper is to present some of the experimental evidence in support of the Master Curve concept and ASTM standard E 1921–97.

## **2. SPECIMEN SIZE EFFECTS IN THE TRANSITION RANGE**

The specimen size effect that has been derived from a weakest-link theory has resulted in the following simple relationship:

$$K_{Jc(1)} = \left( K_{Jc(2)} - 20 \right) \left( \frac{B_2}{B_1} \right)^{\frac{1}{4}} + 20, \quad MPa\sqrt{m}, \quad (1)$$

where

$B_2$  is the thickness of test specimens used to determine toughness  $K_{Jc(2)}$ ,  
 $B_1$  is the thickness of prediction.

This method had been developed on the basis of fractographic evidence of cleavage crack triggering sources (Merkle et al., 1998). However, other specimen size effect models that use competing theories had to be considered during the development of standard method E 1921-97. One competing concept is the “local approach,” which is in essence a variant of the “RKR” postulate (Beremin, 1983), in which cleavage  $K_{Jc}$  is controlled by a critical cleavage stress developing within a certain high-stress location in front of the crack tip. Another competing size effect theory is that the free borders of specimens disrupt the near crack tip stress/strain conditions that would develop normally in infinite bodies. The infinite body condition is referred to as “small-scale yield” (SSY) (Dodds et al., 1997). Finite-element modeling is used to identify and quantify free-border-impacted local crack tip J-integral toughness values. Experimentally determined J-integral values represent a “large-scale yield” (LSY) condition. These LSY-affected toughness values have been presented in parametric form. However, one particular case for the three-point-bend specimen has been mathematically modeled for pressure vessel steels, as follows (Anderson and Dodds, 1991):

$$J_{ssy} = \frac{J_c}{1 + 189 \left( \frac{\sigma_{ys} b_o}{J_c} \right)^{-1.31}}, \quad (2)$$

where

$b_o$  is the initial remaining ligament in the specimen,  
 $J_c$  is the measured J-integral value influenced by LSY conditions,  
 $K_{Jc} = [J_c E]^{1/2}$ .

Equation (2) applies to materials that have a Ramberg-Osgood work-hardening exponent of 10. It is specific to test specimens such as compacts and bend bars that are loaded under dominant bend conditions.

An example comparison of size effect prediction between Eqs (1) and (2) is shown in Fig. 1. The example uses a postulated  $K_{Jc(\text{med})}$  value of 180 MPa√m obtained using 1/2T size specimens. This represents an extreme case to distinctly display the difference in the two methods. Also, a one-to-one proportionality between  $b_o$  and  $B$  is assumed. Figure 1, however, does not show which of the two agrees with experimental evidence. The comparison made with experimental evidence is displayed in Figs. 2 and 3. To prepare these figures, the data were obtained from experiments that had several sizes of specimens tested at one test temperature. A mandatory qualification for acceptable data sets was that at least six 1T specimens had been tested because this would be the reference size for the reference  $K_{Jc(\text{med})}$  value of the demonstration. Values of  $K_{Jc(\text{med})}$  for other specimen sizes were obtained and were converted into 1T equivalent  $K_{Jc(\text{med})}$  values using Eq. (1). These predicted values are plotted in Fig. 2. Figure 3 uses Eq (2) for the same purpose, again keeping in mind that there is a one-to-one proportionality between  $B$  and  $b_o$ .

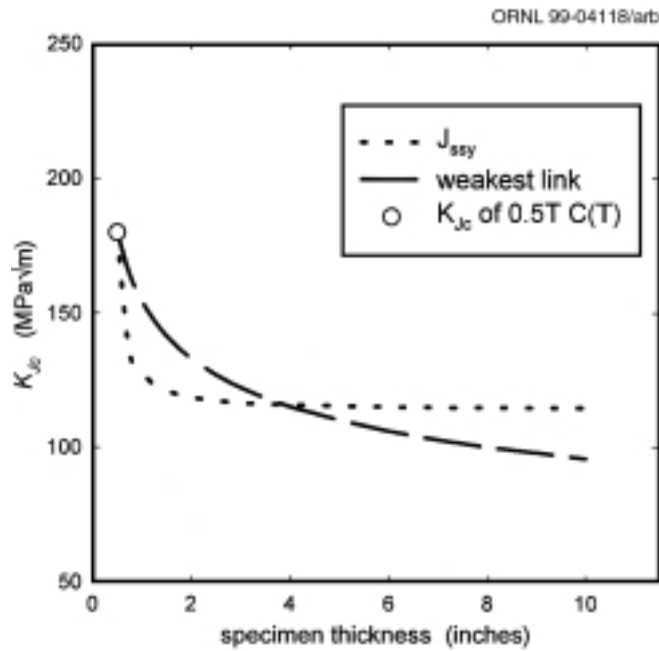


Fig. 1. A comparison of the weakest-link and small-scale size effect models keyed from a  $K_{Jc}$  median toughness value for a 0.5T C(T) specimen.

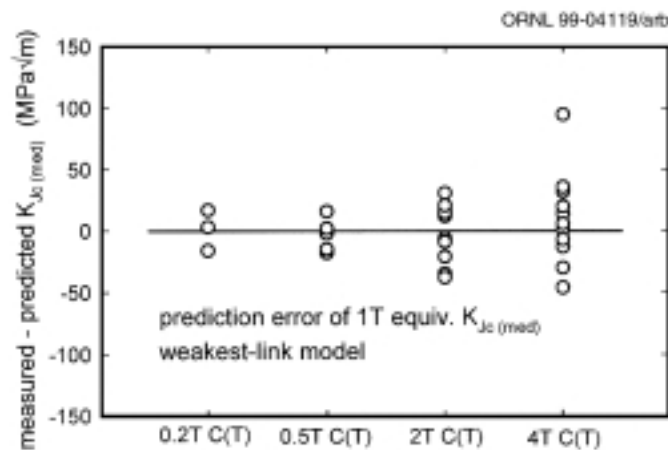


Fig. 2. Prediction error of 1T compact specimen median  $K_{Jc}$  using 0.2T, 0.5T, 2T, and 4T specimen  $K_{Jc}$  values and the weakest-link size effect model.

The rule of at least six replicate specimens could not be used as qualification for tests at other specimen sizes. In particular, 4T size specimens are seldom ever replicated six times, and as few as two replicate tests had to be acceptable for qualification. This added greatly to the variability. Nevertheless, bias shown by the prediction-error distributions provides sufficient evidence for model evaluation. Bias is not evident in Fig. 2. Figure 3 shows some slight bias that suggests that there might be a problem with the SSY stress/strain field free surface effect postulate.

Even though the weakest-link size effect model has performed effectively for size effect adjustments to test data, there is a need to be cautious about extending the use of the model beyond its range of applicability. For example, Eq (1) suggests that when the length of exposed

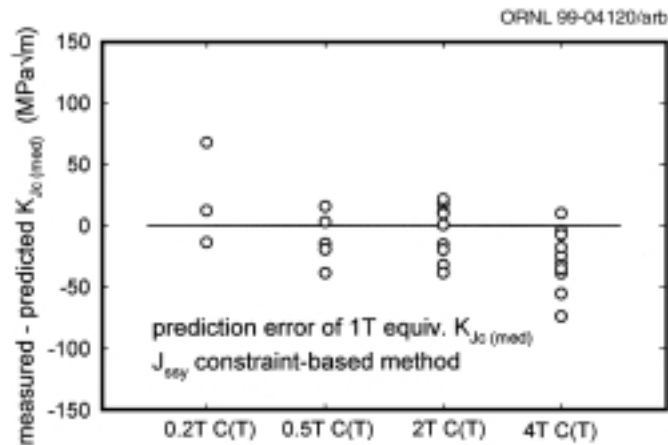


Fig. 3. Prediction error of 1T compact specimen median  $K_{Jc}$  using 0.2T, 0.5T, 2T, and 4T specimen  $K_{Jc}$  values and the small-scale yield model.

crack-front material is extended excessively, it would be possible to reduce the fracture-toughness performance of a material to  $20 \text{ MPa}\sqrt{\text{m}}$ . This is not likely at mid-transition temperatures. McCabe and Merkle (1997) have suggested an idea on how and when this model should be truncated.

Another limitation on the weakest-link model is that the size effect phenomenon will vanish at lower-shelf test temperatures because of a change in the cleavage crack trigger mechanism. The weakest-link mechanism also vanishes as the upper-shelf test temperature is approached. Material toughness on upper shelf is characterized by R-curves, and a great deal of information is on record to show that there is no specimen size effect associated with R-curves (McCabe et al., 1993; McCabe and Ernst, 1983). Hence, the weakest-link effect will gradually vanish as upper shelf is approached. Figures 4 and 5 show why this characteristic of material behavior should not be ignored. Figure 4 has two full R-curves developed on a low upper-shelf material that was tested acceptable data sets was that at least six 1T specimens had been tested because this would be the reference size for the reference  $K_{Jc(med)}$  value of the demonstration. Values of  $K_{Jc(med)}$  for other specimen sizes were obtained and were converted into 1T equivalent  $K_{Jc(med)}$  values using Eq. (1). These predicted values are plotted in Fig. 2. Figure 3 uses Eq (2) for the same purpose, again keeping in mind that there is a one-to-one proportionality between  $B$  and  $b_o$ .

The rule of at least six replicate specimens could not be used as qualification for tests at other specimen sizes. In particular, 4T size specimens are seldom ever replicated six times, and as few as two replicate tests had to be acceptable for qualification. This added greatly to the variability. Nevertheless, bias shown by the prediction-error distributions provides sufficient evidence for (model evaluation. Bias is not evident in Fig. 2. Figure 3 shows some slight bias that suggests that there might be a problem with the SSY stress/strain field free surface effect postulate.

Even though the weakest-link size effect model has performed effectively for size effect adjustments to test data, there is a need to be cautious about extending the use of the model beyond its range of applicability. For example, Eq (1) suggests that when the length of exposed crack-front material is extended excessively, it would be possible to reduce the fracture-toughness performance of a material to  $20 \text{ MPa}\sqrt{\text{m}}$ . This is not likely at mid-transition temperatures. McCabe and Merkle (1997) have suggested an idea on how and when this model should be truncated.

Another limitation on the weakest-link model is that the size effect phenomenon will vanish at lower-shelf test temperatures because of a change in the cleavage crack trigger mechanism. The

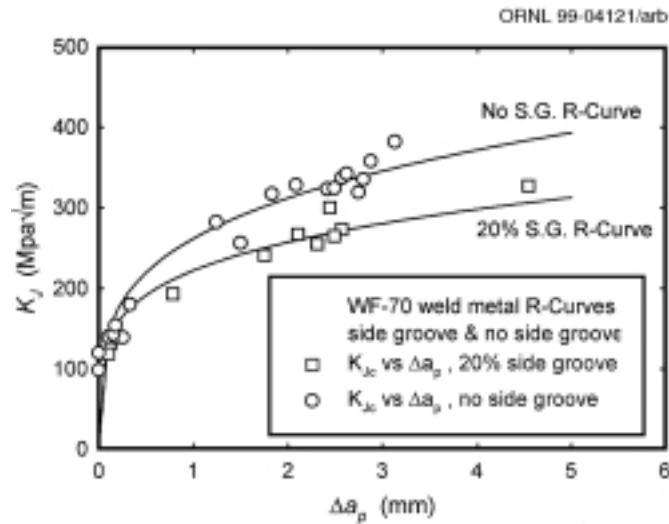


Fig. 4. Upper-shelf R-curves for side-grooved and non-side-grooved low upper-shelf weld metal. Data points are visually measured transition-range stable crack growth,  $\Delta a_p$ , vs  $K_{Jc}$  or  $K_J$  values at test termination.

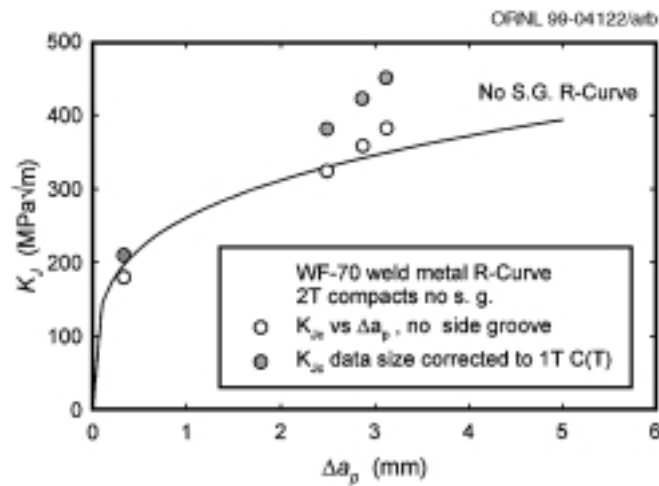


Fig. 5. The effect of size correction to  $K_{Jc}$  values on non-side-grooved 2T specimens when test temperature was within 25°C (45°F) of upper-shelf temperature.

weakest-link mechanism also vanishes as the upper-shelf test temperature is approached. Material toughness on upper shelf is characterized by R-curves, and a great deal of information is on record to show that there is no specimen size effect associated with R-curves (McCabe et al., 1993; McCabe and Ernst, 1983). Hence, the weakest-link effect will gradually vanish as upper shelf is approached. Figures 4 and 5 show why this characteristic of material behavior should not be ignored. Figure 4 has two full R-curves developed on a low upper-shelf material that was tested at a temperature only 25°C (45°F) below the upper shelf. Both tests had to be terminated after full R-curve development at a temperature only 25°C (45°F) below the upper shelf. Both tests had to be terminated after full R-curve development.

The purpose of Fig. 4 is to show that when specimens develop slow-stable crack growth prior to cleavage instability, the fracture properties can be affected by the side-groove practice. The data points shown came from tests made at temperatures that were 4, 25, and 50°C (7.2, 45, and 90°F)

below the upper-shelf temperature. They represent slow-stable crack growth up to the point of cleavage fracture in some cases and the test termination point  $K_J$  values in other cases. Clearly, the specimen side-groove practice can influence  $K_{Jc}$  cleavage values when there is significant slow-stable crack growth. This becomes a problem as upper-shelf temperatures are approached.

Of particular interest are the data obtained from four 2T compact specimens that were not side-grooved. Figure 5 shows separately the data from these specimens before and after adjustment to 1T equivalence. Here, at a test temperature just 25°C (45°F) below the upper-shelf temperature, 0°C, the size correction elevates predicted 1T equivalent toughness to a level greater than the stable crack growth resistance capability of this material. Hence, size correction should not have been used. The HSSI 5th irradiation series had also contained evidence of the vanished weakest-link size effect situation in the case of two 8T size compact specimens tested at a temperature close to the upper shelf temperature (Nanstad et al., 1992). Again, specimen size adjustment to 1T equivalence gave excessively high predicted 1T equivalent fracture toughness. Prior slow-stable crack growth up to onset of cleavage fracture was 0.033 and 0.075 in. (0.84 and 1.9 mm) in the two 8T specimens, giving evidence of the proximity to upper-shelf temperature, whereas most of the other test specimens in that program had negligible prior slow-stable crack growth. Side grooving was not used in the 5th irradiation test series.

### 3. MASTER CURVE

Even though the concept of universal transition curves has been accepted and used in the ASME code for almost 30 years, the concept of one universal median transition curve applicable to one specimen size (Master Curve) has been received with some skepticism. The ASME lower-bound  $K_{Ic}$  curve was established with 11 materials; however, the data from only one of these materials provided the lower values that defined the position and shape of the curve. The ASME lower-bound dynamic  $K_{Ia}$  curve was established with only two materials. Figure 6 represents the data available to verify the Master Curve (Merkle et al., 1998). This plot shows median fracture-toughness values for 18 steels, representing weld metals and base metals, in both unirradiated and irradiated conditions. The curve that seems to fit these median  $K_{Ic}$  values is the Master Curve as defined in ASTM standard method E 1921–97:

$$K_{Jc(\text{med})} = 30 + 70 \exp [0.019 (T - T_0)] \quad \text{MPa} \sqrt{m} \quad , \quad (3)$$

where

$T$  = test temperature,

$T_0$  = reference temperature.

Figure 7 is shown to compare the two methodologies (Sokolov, 1998). The currently used ASME lower-bound  $K_{Ic}$  curve, shown in Fig. 7(a), had utilized only a few of the plotted data points (i.e., the lowest values of  $K_{Ic}$ ) to arrive at a transition curve shape. Despite the apparent basis of eight materials, the HSST plate 02 data seem to have controlled the lower-bound curve development. The Master Curve method as applied to setting lower-bound coverage is shown in Fig. 7(b), along with the ASME curve. In the case of the lower bound derived from the Master Curve, all of the data shown were used to arrive at a transition-curve position. For the ASME curve to be close to a lower bound, a reference temperature based on  $T_0$  was used. A 35°F (19.4°C) margin had to be added.

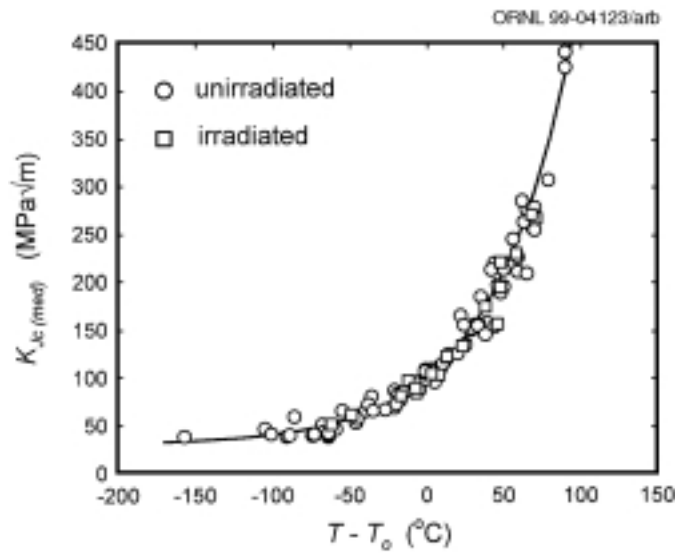


Fig. 6. Currently accumulated median  $K_{Ic}$  transition-range data for 18 materials plotted with the ASTM E1921-97 Master Curve.

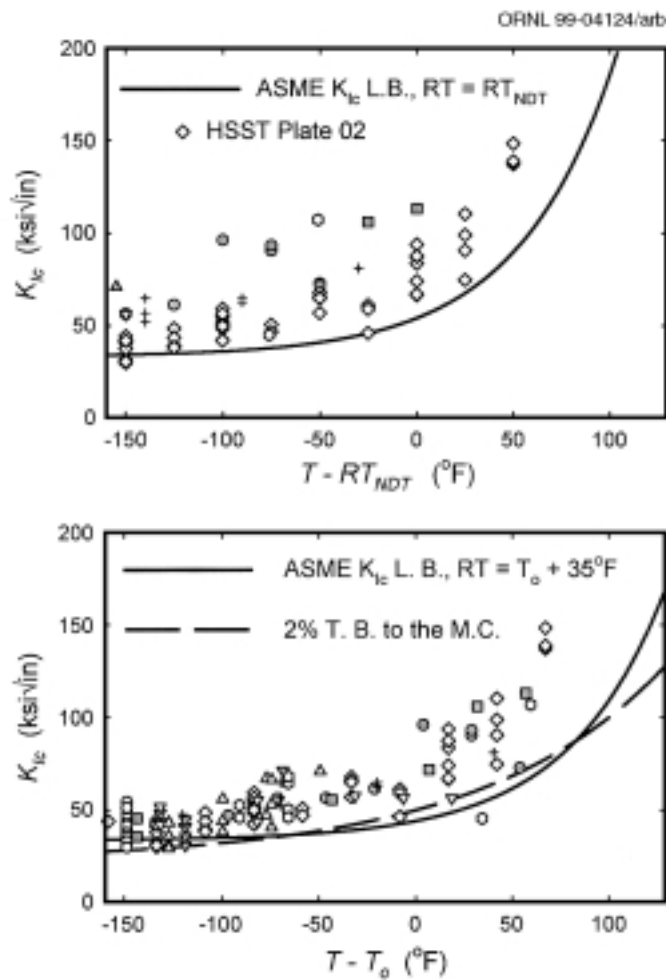


Fig. 7. Comparison of lower bounding of the (a) EPRI  $K_{Ic}$  data base values and (b) comparing the ASME method vs the Master Curve method.



In the draft ASME code case for replacing  $RT_{NDT}$  with  $RT_{T_0}$  determined by the Master Curve procedure,  $RT_{T_0}$  is calculated by adding 35°F (19.4°C) to  $T_0$ . A technical basis document pertaining to applications of the Master Curve approach has been published (EPRI, 1998), but exactly how the 35°F (19.4°C) temperature shift was selected is not explained.

Sokolov and Nanstad (1999) examined data from irradiated materials to determine the effect of irradiation damage on the Master Curve shape (see Fig. 8). In this case, each datum is plotted instead of median values as in Fig. 6. Least-squares curve fitting was applied to find the best curve shape. The best fit had a coefficient inside of the Eq. (3) exponential term set at 0.017. When linear regression is used on the Fig. 6 data, the best coefficient is 0.018. In both cases, the differences were not significant from a practical point of view, and alteration of Eq. (3) is not necessary for the irradiated data examined.

#### 4. DEVELOPMENT OF $T_0$ FROM PRECRACKED CHARPY SPECIMENS

The observation of a weakest-link behavior in steels coupled with elastic-plastic analysis methods has permitted a large reduction in specimen size requirements so that specimens of practical size for laboratory testing can now be used. A practical specimen size for surveillance capsule work is defined as the precracked Charpy specimen. The rationale for this assertion is that in many cases surveillance capsules contain only Charpy and tensile specimens, and only Charpy specimens are currently available for fracture-toughness evaluations. However, the precracked Charpy specimen is of marginal size to be a viable specimen for the development of fracture-mechanics data. The challenge of developing test procedures to produce viable data from such specimens has been undertaken in several projects by various groups. This work is currently in progress, and only preliminary evidence is available at the present time. Figure 9 summarizes the present accumulation by the authors of available information. There is sufficient cause for optimism, but it is premature to conclude that  $T_0$  temperatures can be determined from such small specimens without modification to the test procedure. Figure 9 appears to show some bias tendencies because most of the Charpy-generated  $T_0$  values appear to be on the high-toughness side of the one-to-one correlation line.

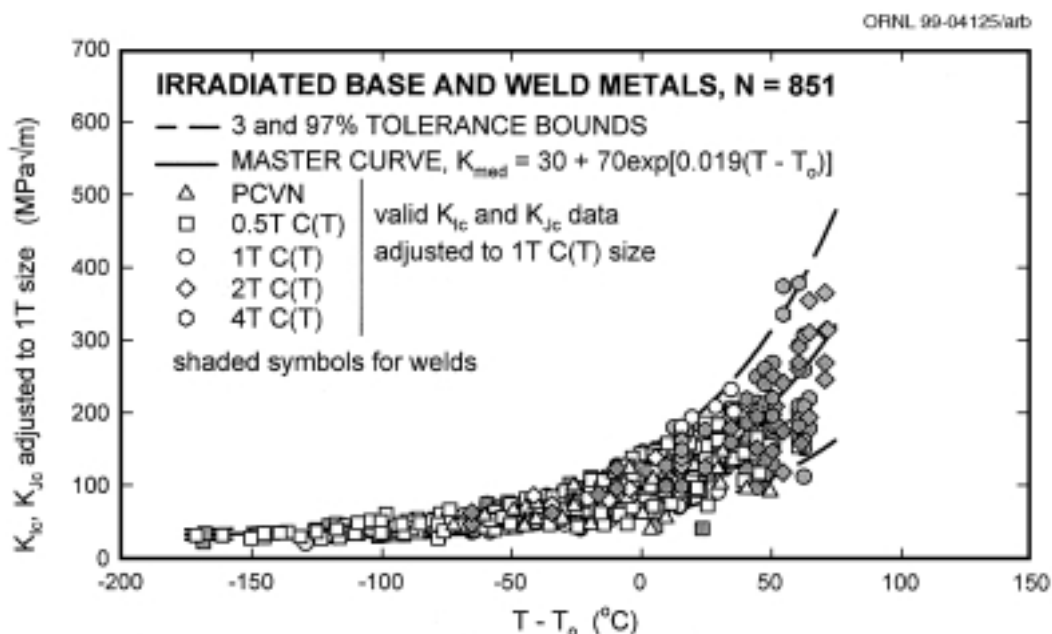


Fig. 8. The irradiated fracture-toughness data size-adjusted to 1T equivalence and normalized to  $T_0$  with the Master Curve and 3% and 97% tolerance bounds. Valid data only.

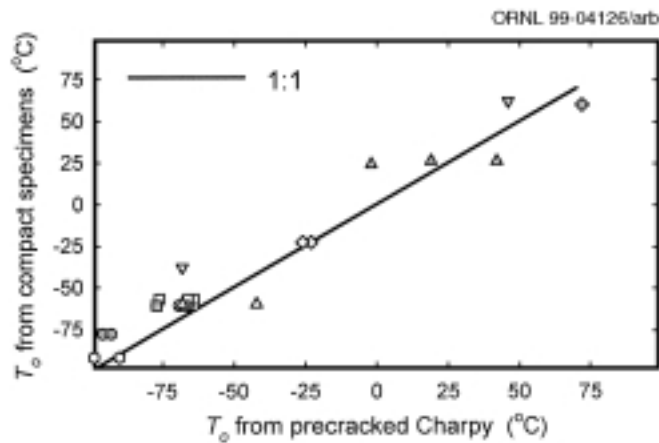


Fig. 9. Comparison of reference temperature,  $T_0$ , determination. Compact specimens vs precracked Charpys.

## 5. CONCLUSION

Specimen size effects developed in the mid-transition range are most accurately defined by the model derived from weakest-link theory. The mechanism tends to break down at lower-shelf temperatures and at temperatures approaching upper shelf. Specimen size effects tend to vanish as these two conditions are approached.

The Master Curve method of defining ductile-to-brittle behavior of steels has advanced the concept of universal transition curves from speculation to a concept that is supported by theoretical reasoning and proven with ample supporting experimental data. The ASME code has been relying on a universal fracture-toughness curve concept as a working postulate for almost 30 years. The present Master Curve finding suggests that the ASME lower-bound  $K_{Ic}$  curve does not have the correct shape. Size effects on fracture toughness and the effect of irradiation damage on transition-curve shape have been unresolved issues for the ASME code curves. The refinement of curve shape definition through introduction of the Master Curve concept has permitted a more accurate evaluation of irradiation damage effects on universal curve shape. For the data base evaluated, the current evidence is that curve shape does not change as a consequence of irradiation.

The precracked Charpy specimen is currently being evaluated as a potentially viable fracture-mechanics specimen. Although there is insufficient evidence for a final conclusion, some bias in  $T_0$  prediction appears to be likely.

### *Acknowledgments*

Research sponsored by the Division of Engineering Technology, Office of Nuclear Regulatory Research, U.S. Nuclear Regulatory Commission, under Interagency Agreement DOE 1886-N695-3W with the U.S. Department of Energy under Contract DE-AC05-96OR22464 with Lockheed Martin Energy Research Corporation.

## REFERENCES

American Society for Testing and Materials, 1982a, "Standard test method for plane strain fracture toughness of metallic materials," Annual Book of ASTM Standards, Part 10, E 399-81.

American Society for Testing and Materials, 1982b, "Standard method for conducting drop-weight test to determine nil-ductility transition temperature of ferritic steels," Annual Book of ASTM Standards, Part 10, E 208-81.

American Society for Testing and Materials, 1998, "Standard test method for determination of reference temperature,  $t_0$ , for ferritic steels in the transition range," Annual Book of ASTM Standards, Vol. 03.01, E 1921-97.

American Society of Mechanical Engineers, 1993, "Fracture toughness requirements for material," asme boiler and pressure vessel code, Sect. III, NB 2300, NB-2321.1 & NB-2321.2.

Anderson, T. L., and Dodds, R.H., Jr., 1991, "Specimen size requirements for fracture toughness testing in the ductile brittle transition region," Journal of Testing and Evaluation, Vol. 19, pp. 123-34.

Beremin, F. M., 1983, "A local criterion for cleavage fracture of a nuclear pressure vessel steel," Metallurgical Transactions, 14A, pp. 2277-87.

Dodds, R. H., Jr., Ruggieri, C., and Koppenhoefer, K. C., 1997, "3D effects on models for transferability of cleavage fracture toughness," ASTM STP 1321, American Society for Testing and Materials, pp. 179-97.

Electric Power Research Institute, 1993, "White paper on reactor vessel integrity requirements for level a and b conditions," ASME Section XI Task Group on Reactor Vessel Integrity Requirements Final Report, EPRI TR-100251, Electric Power Research Institute, Palo Alto, CA.

Electric Power Research Institute, 1998, "Application of Master Curve fracture toughness methodology for ferritic steels," TR-108390, Electric Power Research Institute, Palo Alto, CA.

Landes, J. D., and Shaffer, D. H., 1980, "Statistical characterization of fracture in the transition region," ASTM STP 700, American Society for Testing and Materials, pp. 368-82.

McCabe, D. E., and Ernst, H. A., 1983, "A perspective on r-curves and instability theory," ASTM STP 791, Vol. 1, American Society for Testing and Materials, pp. 561-84.

McCabe, D. E., Landes, J. D., and Ernst, H. A., 1983, "An evaluation of the  $j_r$ -curve method for fracture toughness characterization," ASTM STP 803, Vol. II, American Society for Testing and Materials pp. 562-81.

McCabe, D. E., and Merkle, J. G., 1997, "Estimation of lower-bound  $K_{Jc}$  on pressure vessel steels from invalid data," ASTM STP 1321, American Society for Testing and Materials, pp. 198-213.

Merkle, J. G., Wallin, K., and McCabe, D. E., 1998, "Technical basis for an ASTM standard on determining the reference temperature,  $T_o$ , for Ferritic Steels in the Transition Range," NUREG/CR-5504, U.S. Nuclear Regulatory Commission.

Nanstad, R. K., Haggag, F. M., McCabe, D. E., Iskander, S. K., Bowman, K. O., and Menke, B. H., 1992, "Irradiation effects on fracture toughness of two high-copper submerged-arc welds, HSSI Series 5," NUREG/CR 5913, Vol. 1, U. S. Nuclear Regulatory Commission.

Sokolov, M. A., 1998, "Statistical analysis of the ASME  $K_{Ic}$  data base," Transactions of the ASME, Vol. 120, pp. 24–27.

Sokolov, M. A., and Nanstad, R. K., 1999, "Comparison of irradiation-induced shifts of  $K_{Ic}$  and Charpy impact toughness for reactor pressure vessel steels," Effects of Radiation on Materials: 18<sup>th</sup> International Symposium, ASTM STP 1325, American Society for Testing and Materials, pp. 167–90.

Wallin, K., 1989, "A simple theoretical Charpy V- $K_{Ic}$  correlation for irradiation embrittlement," 1989 PVP/JSME Cosponsored Conference, PVP Vol. 170, pp. 93–100.

Welding Research Council, 1972, "PVRC recommendations on toughness requirements for ferritic materials," ad hoc group on toughness requirements, WRC Bulletin 175.